

Conformal-thin-sandwich initial data for a single boosted or spinning black hole puncture

Pablo Laguna

*Center for Gravitational Physics and Geometry,
Center for Gravitational Wave Physics,
Department of Astronomy and Astrophysics,
Department of Physics,
Penn State University, University Park, PA 16802*

Sequences of initial-data sets representing binary black holes in quasi-circular orbits have been used to calculate what may be interpreted as the innermost stable circular orbit. These sequences have been computed with two approaches. One method is based on the traditional conformal-transverse-traceless decomposition and locates quasi-circular orbits from the turning points in an effective potential. The second method uses a conformal-thin-sandwich decomposition and determines quasi-circular orbits by requiring the existence of an approximate helical Killing vector. Although the parameters defining the innermost stable circular orbit obtained from these two methods differ significantly, both approaches yield approximately the same initial data, as the separation of the binary system increases. To help understanding this agreement between data sets, we consider the case of initial data representing a single boosted or spinning black hole puncture of the Bowen-York type and show that the conformal-transverse-traceless and conformal-thin-sandwich methods yield identical data, both satisfying the conditions for the existence of an approximate Killing vector.

PACS numbers: 04.30+x

I. INTRODUCTION

Binary systems involving compact objects such as black holes and neutron stars have been the main source of attention of numerical relativists in the past two decades. The motivation for studying these systems has been enhanced by the urgency of producing results that could help observational efforts like LIGO, GEO600, TAMA300 and VIRGO [1]. Unfortunately the problem of producing complete and sufficiently accurate numerical simulations of orbits and mergers of compact binaries is still not feasible. This impediment does not imply that the results produced so far are devoid of any astrophysical relevance. Simulations of a few orbits of neutron star binaries have been obtained [2, 3]. Grazing collisions and wave forms produced from the final plunge of a binary black hole system have been also computed [4]. And of direct relevance to the work presented in this paper is the study of the behavior of binary orbits using sequences of initial data configurations.

Astrophysically realistic initial data sets representing black hole binaries are crucial. Without them, the predictive power of gravitational wave source simulations, with relevance to data analysis efforts, is seriously compromised. Constructing initial data sets involves a series of choices such as conformal transformations, tensor decompositions, topologies, boundary conditions, freely specifiable data to name a few. These choices have a profound effect on the physical properties of the data.

Two general approaches for constructing initial data are currently under consideration. The oldest approach has its roots in the work by Lichnerowicz and York [5]. This approach is based on conformal transformations and transverse-traceless (CTT) decompositions. The sec-

ond and most recent approach, currently receiving considerable attention, attempts to establish a more direct “space-time” connection. It borrows some of the ideas from the CTT method, namely conformal transformations and traceless decompositions, but in addition provides a natural framework for setting up quasi-equilibrium configurations of binary systems. Under this approach, initial data can be viewed as derived from a “thick slice or thin sandwich” section of the space-time. The method was pioneered by Mathews and Wilson [6]; recently used by Grandclément, Gourgoulhon and Bonazzola [7]; and formally characterized by York [8]. Because the approach also involves conformal transformations, it is known as the conformal thin-sandwich (CTS) method.

Initial data sets representing binaries in quasi-circular orbits will be needed as a starting point of any evolution simulation aimed at producing gravitational waveforms of astrophysical black hole binaries. Cook [9] introduced the first method to locate what could be identified as black hole binaries in quasi-circular orbits. The method, called the effective potential method, is based on the potential

$$E_b = E - 2M, \quad (1.1)$$

where E_b represents the binding energy of the system, E the total energy and M the irreducible mass of each individual black hole. The total energy E is a well defined quantity, namely the total ADM mass [10]. However, defining individual black hole masses for interacting black holes is not a completely well defined concept [11]. Nonetheless, a reasonable approximation is to assume that the irreducible mass is given by the proper area of the apparent horizon. Quasi-circular orbits are

then found from the condition

$$\left. \frac{\partial E_b}{\partial l} \right|_{M,J} = 0, \quad (1.2)$$

where l is the proper separation of the horizons and J the total angular momentum of the binary. Similarly, the angular velocity Ω is found from

$$\Omega = \left. \frac{\partial E_b}{\partial J} \right|_{M,l}. \quad (1.3)$$

Given this approach to identifying quasi-circular orbits, the innermost stable circular orbit (ISCO) is found by looking at the end point of a sequence of quasi-circular orbits.

Baumgarte [12] and later Baker [13] recomputed, using Cook's effective potential method, quasi-circular orbit sequences. One of the motivations for this work was to investigate whether Cook's results were sensitive to how the black hole singularities are handled. Instead of using a topology requiring conformal-imaging as used by Cook [9], Baumgarte and Baker handled the black hole singularities via the puncture method [14]. Both studies produced results in close agreement with those by Cook. In the remainder of this paper, quasi-circular orbit data sets computed with the CTT method will be referred as Cook-Baumgarte-Baker (CBB) data sets.

As mentioned before, the CTS approach has also been used byourgoulhon, Grandclément and Bonazzola (GGB) [7, 15] to construct quasi-circular orbits of black hole binary systems. The essence of this work is to identify quasi-circular orbits based on the assumption that the space-time possesses an approximate helical Killing vector. One important aspect of the GGB sequences is that they yield an ISCO identification in better agreement with post-Newtonian results [16] when compared with CBB sequences. Specifically, the normalized binding energy $e = E/2M - 1$ at the ISCO from post-Newtonian estimates is $e \approx -1.67\%$. The GGB study yields $e \approx -1.73\%$. On the other hand, the CBB estimate is significantly more strongly bound, $e \approx -2.3\%$. These differences show more dramatically when comparing the ISCO orbital period. Post-Newtonian calculations yield $T/2M \approx 71.2$ and in the GGB work $T/2M \approx 62.8$. In contrast, the CBB data estimate $T/2M \approx 37$.

Reasons for these discrepancies are not completely understood. One suggestion was that these differences were due to the criteria for identifying quasi-circular orbits. Instead of the method used by CBB described above, GGB determined the co-rotating frame defining quasi-circular orbits from the requirement that the ADM and Komar [17] masses are equal. The motivation for this choice was that the Komar and ADM masses only agree for stationary space-times. Therefore, the data computed this way have a better chance of representing a quasi-stationary situation. Skoge and Baumgarte [18] designed a simple example involving thin-spherical shells of collision-less particles in circular orbits which shows that the effective potential method and the equal Komar

and ADM masses method for identifying circular orbits are equivalent. More recently, Tichy and Brüggmann [19] computed sequences of CTS binary black hole punctures that yield a similar conclusion. These studies provide strong support to the view that the differences between CBB and GGB data sets are not due to the method for identifying quasi-circular orbits but somewhere else.

Another possible explanation for the ISCO discrepancy that has been mentioned is once again the approach to representing the black hole singularities. The GGB initial data sequences are based on a topology requiring conformal-imaging [9]. The work in Refs. [19, 20] was mostly aimed at testing this by extending the GGB results to the case of black holes represented by punctures. Unfortunately, the data obtained in this work only approximately satisfied one of the conditions used by GGB to define quasi-stationarity. Recently, Hannam and collaborators [21] pointed out the serious difficulties in constructing CTS binary data in quasi-equilibrium based on punctures instead of conformal-imaging.

There is however an important aspect of the CBB and GGB sequences that cannot be ignored. In spite of their differences for determining the ISCO, the CBB and GGB sequences show a close agreement when the separation of the binary systems increases. Therefore, at large separations, it should be possible to translate CBB into GGB data and vice-versa, independently of the procedure used to represent the black holes. The work in this paper is motivated by this observation. Since for large binary separations the black holes are approximately isolated, we focus attention on single boosted or spinning black hole punctures. We demonstrate that it is possible to translate the CTT data into a CTS form while preserving the conditions used by GGB, namely the existence of an approximate Killing vector, thus circumventing in these cases the problems pointed out in Ref. [21].

The paper is organized as follows. In Sec. II, the conformal decomposition of the Einstein constraints is presented up to the point where the CTT and CTS methods agree. Brief reviews of the CTT and CTS methods are presented in Secs II A and II B, respectively. The conditions necessary for translating between CTT and CTS data are derived in Sec. III. The main results regarding boosted or spinning punctures are presented in Sec. IV. Conclusions are given in Sec. V.

II. DECOMPOSITION OF THE CONSTRAINTS

Under the standard 3+1 decomposition of the Einstein equations, the 4-dimensional line element is written as

$$ds^2 = -\alpha^2 dt^2 + \tilde{g}_{ij} (dx^i + \beta^i dt) (dx^j + \beta^j dt), \quad (2.1)$$

with \tilde{g}_{ij} the intrinsic 3-metric to Σ_t ($t = \text{constant}$ hypersurfaces), α the lapse function and β^i the shift vector.¹ The extrinsic curvature of Σ_t is defined by

$$\tilde{K}_{ij} \equiv -\frac{1}{2} \mathcal{L}_N \tilde{g}_{ij}, \quad (2.2)$$

with \mathcal{L}_N the Lie derivative along the unit time-like normal N^μ to Σ_t . In terms of these variables, the vacuum Einstein equations consist [10] of a set of evolution equations:

$$\partial_o \tilde{g}_{ij} = -2\alpha \tilde{K}_{ij} \quad (2.3)$$

$$\begin{aligned} \partial_o \tilde{K}_{ij} &= -\tilde{\nabla}_i \tilde{\nabla}_j \alpha + \alpha \tilde{R}_{ij} \\ &+ \alpha (\tilde{K} \tilde{K}_{ij} - 2 \tilde{K}_{ik} \tilde{K}^k{}_j), \end{aligned} \quad (2.4)$$

and a set of constraint equations:

$$\tilde{R} + \tilde{K}^2 - \tilde{K}_{ij} \tilde{K}^{ij} = 0 \quad (2.5)$$

$$\tilde{\nabla}_j \tilde{K}^{ij} - \tilde{\nabla}^i \tilde{K} = 0. \quad (2.6)$$

Above, $\tilde{\nabla}_i$ and \tilde{R}_{ij} denote respectively covariant differentiation and Ricci tensor associated with \tilde{g}_{ij} . Also $\tilde{K} \equiv \tilde{g}^{ij} \tilde{K}_{ij}$, $\tilde{R} \equiv \tilde{g}^{ij} \tilde{R}_{ij}$ and $\partial_o \equiv \partial_t - \mathcal{L}_\beta$.

Constructing initial data involves specifying $(\tilde{g}_{ij}, \tilde{K}_{ij})$ on a given Σ_t subject to the four constraint equations (2.5) and (2.6). In other words, out of the twelve pieces in $(\tilde{g}_{ij}, \tilde{K}_{ij})$, only eight are freely specifiable. The remaining four are fixed by these constraints. Thus, setting up the initial data problem in general relativity becomes the task of singling out in $(\tilde{g}_{ij}, \tilde{K}_{ij})$ those quantities that will be fixed by the constraints. This is accomplished via conformal transformations and tensorial decompositions. The CTT and CTS approaches are examples of this methodology.

Both the CTT and CTS methods involve applying a conformal transformation of the 3-metric and a decomposition of the extrinsic curvature of the form:

$$\tilde{g}_{ij} = \phi^4 g_{ij} \quad (2.7)$$

$$\tilde{K}_{ij} = \tilde{A}_{ij} + \frac{1}{3} \tilde{g}_{ij} K, \quad (2.8)$$

such that $\tilde{A}^i{}_i = 0$. Notice that the choice $\tilde{K} = K$ has been made. In terms of these new variables, the constraint equations (2.5) and (2.6) become:

$$\phi^{-4} R - 8\phi^{-5} \nabla^2 \phi + \frac{2}{3} K^2 - \tilde{A}_{ij} \tilde{A}^{ij} = 0 \quad (2.9)$$

$$\nabla_j \tilde{A}^{ij} + 10 \tilde{A}^{ij} \nabla_j \ln \phi - \frac{2}{3} \phi^{-4} \nabla^i K = 0, \quad (2.10)$$

where ∇_i and R denote respectively covariant differentiation and Ricci scalar associated with the conformal

3-metric g_{ij} . In deriving Eq. (2.10), we have used the following identity:

$$\tilde{\nabla}_j \tilde{T}^{ij} = \phi^n [\nabla_j T^{ij} + (10+n) T^{ij} \nabla_j \ln \phi], \quad (2.11)$$

where $\tilde{T}^{ij} = \phi^n T^{ij}$, with n an exponent. Similarly, the evolution equations (2.3) and (2.4) can be rewritten as:

$$\partial_t \phi = \beta^i \nabla_i \phi + \frac{1}{6} \phi (\nabla_i \beta^i - \alpha K) \quad (2.12)$$

$$\partial_t g_{ij} = (\mathbb{L}\beta)_{ij} - 2\alpha \phi^{-4} \tilde{A}_{ij} \quad (2.13)$$

$$\partial_o K = -\tilde{\nabla}^2 \alpha + \alpha \left(\tilde{A}^{ij} \tilde{A}_{ij} + \frac{1}{3} K^2 \right) \quad (2.14)$$

$$\begin{aligned} \partial_o \tilde{A}_{ij} &= [-\tilde{\nabla}_i \tilde{\nabla}_j \alpha + \alpha \tilde{R}_{ij}]^{TF} \\ &- \alpha \left(2 \tilde{A}_{ik} \tilde{A}^k{}_j + \frac{1}{3} K \tilde{A}_{ij} \right) \end{aligned} \quad (2.15)$$

where the superscript TF denotes the trace-free part of the tensor within square brackets and

$$(\mathbb{L}\beta)_{ij} \equiv 2 \nabla_{(i} \beta_{j)} - \frac{2}{3} g_{ij} \nabla_k \beta^k. \quad (2.16)$$

Since we are focusing our attention on the methodologies followed by CBB and GGB, we introduce at this point the assumptions that both share, namely conformal flatness $g_{ij} = \eta_{ij}$ and vanishing of K . These two conditions exhaust six of the eight freely specifiable quantities in $(\tilde{g}_{ij}, \tilde{K}_{ij})$. Under these assumptions, Eqs. (2.9) and (2.10) reduce to:

$$\nabla^2 \phi + \frac{1}{8} \phi^5 \tilde{A}_{ij} \tilde{A}^{ij} = 0 \quad (2.17)$$

$$\nabla_j \tilde{A}^{ij} + 10 \tilde{A}^{ij} \nabla_j \ln \phi = 0. \quad (2.18)$$

In the remainder of the paper, we will continue referring to the approach followed by CBB as CTT and by GGB as CTS, but one should keep in mind that CTT and CTS are more general. They do not necessarily require conformal flatness nor $K = 0$.

A. Conformal-Transverse-Traceless Decomposition

The CTT method was pioneered by York and collaborators [5]. Until recently, CTT has been the preferred method to construct initial data in numerical relativity. Given Eqs. (2.17) and (2.18), one introduces the following conformal transformation and transverse-longitudinal decomposition of the extrinsic curvature:

$$\begin{aligned} \tilde{A}^{ij} &= \hat{\phi}^{-10} \hat{A}^{ij} \\ &= \hat{\phi}^{-10} [\Theta^{ij} + (\mathbb{L}W)^{ij}], \end{aligned} \quad (2.19)$$

such that $\nabla_j \Theta^{ij} = 0$ and $\Theta^i{}_i = 0$. We label CTT quantities with hats.

Here Θ^{ij} represents the transverse part of \hat{A}^{ij} . Since Θ^{ij} is trace and divergence free, it contains the two

¹ Latin indices denote 3-dimensional spatial indices and Greek indices 4-dimensional space-time indices.

remaining freely specifiable pieces of the initial data $(\hat{g}_{ij}, \hat{K}_{ij})$. The longitudinal part of \hat{A}^{ij} is given by $(\mathbb{L}W)^{ij}$. It is this part of \hat{A}^{ij} that is fixed by the momentum constraint (2.18). Furthermore, it is not difficult to show that Θ^{ij} and $(\mathbb{L}W)^{ij}$ satisfy the following orthogonality condition:

$$\int_{\Sigma_t} \Theta^{ij} (\mathbb{L}W)_{ij} \sqrt{\eta} d^3x = 0. \quad (2.20)$$

For simplicity CBB assumed that $\Theta^{ij} = 0$. Therefore, substitution of (2.19) into (2.17) and (2.18) yields:

$$\nabla^2 \hat{\phi} + \frac{1}{8} \hat{\phi}^{-7} (\mathbb{L}W)^2 = 0 \quad (2.21)$$

$$\nabla_j (\mathbb{L}W)^{ij} = 0, \quad (2.22)$$

where we have introduced the notation $(\mathbb{L}W)^2 \equiv (\mathbb{L}W)^{ij} (\mathbb{L}W)_{ij}$. In summary, the initial data problem under the CTT approach reduces to solving first Eq. (2.22) for W^i and then using this solution to solve for $\hat{\phi}$ from Eq. (2.21).

Bowen and York [22] found solutions to the momentum constraint (2.22) representing single black holes with linear momentum P^i or angular momentum J^i . Specifically,

$$W^i = -\frac{1}{4r} (7P^i + n^i n_j P^j) \quad (2.23)$$

$$W^i = -\frac{1}{r^2} \epsilon^{ijk} J_j n_k, \quad (2.24)$$

with n^i the unit normal of constant r spheres in flat space; namely, $n^i = (x, y, z)/r = (\partial/\partial r)^i$ and $r = \|x^i\|$. In terms of the solutions (2.23) and (2.24), the extrinsic curvature \hat{A}^{ij} takes the form:

$$\hat{A}^{ij} = \frac{3}{2r^2} \left[2P^{(i} n^{j)} - (\eta^{ij} - n^i n^j) n_k P^k \right] \quad (2.25)$$

$$\hat{A}^{ij} = \frac{6}{r^3} n^{(i} \epsilon^{j)kl} J_k n_l. \quad (2.26)$$

Given the solution with linear momentum (2.25), solutions representing non-spinning binary black holes are obtained via the following superposition:

$$\hat{A}^{ij} = \hat{A}^{ij}(C_1^k, P_1^k) + \hat{A}^{ij}(C_2^k, P_2^k), \quad (2.27)$$

where C_A^i with $A = 1, 2$ denotes the coordinate location of each of the black holes. The explicit expression for $\hat{A}^{ij}(C_A^i, P_A^i)$ is given by (2.25) with $r_A = \|x^i - C_A^i\|$ and $n_A^i = (x^i - C_A^i)/r_A$. It is not difficult to show that, with \hat{A}^{ij} given by (2.27), the total ADM linear and angular momentum (about the origin of the coordinate system) are $P^i = P_1^i + P_2^i$ and $J_i = \epsilon_{ijk} (C_1^j P_1^k + C_2^j P_2^k)$, respectively.

CBB specialized to the case of equal mass black holes, in the center-of-momentum frame of the binary system and in quasi-circular orbit. Thus, $P^i \equiv P_1^i = -P_2^i$ and $P_i C^i \equiv P_i (C_1^i - C_2^i) = 0$. In addition, asymptotic flatness requires that in solving the Hamiltonian constraint

(2.21) one imposes the following Robin boundary condition as $r \rightarrow \infty$:

$$n^i \nabla_i \hat{\phi} = \frac{(1 - \hat{\phi})}{r}. \quad (2.28)$$

The differences between the procedures followed by Cook [9] and by Baumgarte [12] and Baker [13] entered in the approach used to handle the black hole singularities. Cook [9] used the conformal-imaging approach. Baumgarte [12] and Baker [13], on the other hand, applied the puncture method developed by Brandt and Brügmann [14]. Constructing sequences of initial data sets reduces then to a 3-dimensional parameter space consisting of $C \equiv \|C^i\|$, $P \equiv \|P^i\|$ and a third parameter. For the conformal-imaging approach method the third parameter is related to the radius of the throat of the black holes and for the puncture method to their ‘‘bare’’ mass.

B. Conformal-Thin-Sandwich Decomposition

The fundamental difference between the CTT method used by GGB and the CTS method used by CBB lies in the decomposition of the extrinsic curvature. Instead of using (2.19), one introduces

$$\begin{aligned} \tilde{A}^{ij} &= \bar{\phi}^{-4} \bar{A}^{ij} \\ &= \bar{\phi}^{-4} \frac{1}{2\alpha} [-u^{ij} + (\mathbb{L}\beta)^{ij}], \end{aligned} \quad (2.29)$$

where bars will be used to denote CTS quantities.

The first aspect to notice is that, strictly speaking, $(\mathbb{L}\beta)^{ij}/2\alpha$ and $u^{ij}/2\alpha$ cannot be viewed respectively as the longitudinal and transverse parts of \bar{A}^{ij} . That is, they do not satisfy the orthogonality condition (2.20). In Ref. [23], the measure used in (2.20) is modified to show that it is possible to arrive to a orthogonal decomposition of \bar{A}^{ij} of the form

$$\bar{A}^{ij} = \Theta^{ij} + \frac{1}{2\alpha} (\mathbb{L}B)^{ij}, \quad (2.30)$$

with $\nabla_j \Theta^{ij} = \Theta^i_i = 0$. The orthogonality condition in this case reads

$$\begin{aligned} \int_{\Sigma_t} \Theta^{ij} \frac{1}{2\alpha} (\mathbb{L}B)_{ij} 2\alpha \sqrt{\eta} d^3x = \\ \int_{\Sigma_t} \Theta^{ij} (\mathbb{L}B)_{ij} \sqrt{\eta} d^3x = 0. \end{aligned} \quad (2.31)$$

The next step in the CTS approach is to realize that the freely specifiable nature of u_{ij} can be exploited to find quasi-equilibrium configurations. From the evolution equation (2.13) one has that

$$\partial_t \bar{g}_{ij} = (\mathbb{L}\beta)_{ij} - 2\alpha \bar{A}_{ij} = u_{ij}. \quad (2.32)$$

For quasi-equilibrium configurations defined by an approximate helical Killing vector, it is then natural to choose $u_{ij} = 0$.

With $u_{ij} = 0$, the Hamiltonian and momentum constraint equations (2.17) and (2.18) read

$$\nabla^2 \bar{\phi} + \frac{\bar{\phi}^5}{32\alpha^2} (\mathbb{L}\beta)^2 = 0 \quad (2.33)$$

$$\nabla_j (\mathbb{L}\beta)^{ij} - (\mathbb{L}\beta)^{ij} \nabla_j \ln(\alpha \bar{\phi}^{-6}) = 0. \quad (2.34)$$

Because of the particular form used to decompose \bar{A}_{ij} in (2.29), a recipe for fixing α is also needed. Since one of the assumptions used is $K = 0$, it is natural to require for Σ_t to be a maximal slice, namely $\partial_t K = 0$. Substitution of $K = \partial_t K = 0$ into the evolution equation (2.14) yields

$$\nabla^2 \alpha + 2\bar{\phi}^{-1} \nabla_i \bar{\phi} \nabla^i \alpha = \frac{\bar{\phi}^4}{4\alpha} (\mathbb{L}\beta)^2, \quad (2.35)$$

from which one can solve for α . It is convenient to rewrite (2.35) with the help of Eq. (2.33) as follows:

$$\nabla^2(\alpha\bar{\phi}) - \frac{7}{32} \frac{\bar{\phi}^6}{(\alpha\bar{\phi})} (\mathbb{L}\beta)^2 = 0. \quad (2.36)$$

Notice from (2.12) and (2.15) that choosing $u_{ij} = 0$, $\partial_t K = 0$ and $K = 0$ does not necessarily imply that $\partial_t \bar{\phi} = 0$ nor $\partial_t \bar{A}_{ij} = 0$, which would be necessary in order to have an exact helical Killing vector.

The boundary conditions needed to solve Eqs. (2.33), (2.34) and (2.35) are that as $r \rightarrow \infty$,

$$n^i \nabla_i \alpha = \frac{(1-\alpha)}{r} \quad (2.37)$$

$$n^i \nabla_i \bar{\phi} = \frac{(1-\bar{\phi})}{r} \quad (2.38)$$

$$\beta^i \rightarrow \Omega \left(\frac{\partial}{\partial \varphi_o} \right)^i, \quad (2.39)$$

with Ω the orbital angular velocity of the binary and $(\partial/\partial \varphi_o)^i$ the Killing vector of the flat metric for rotation in the φ_o direction. In the GGB set up, the black holes are represented by two sheets of the Misner-Lindquist manifold (see [7] for details). That is, there are two throats S_1 and S_2 of radii a_1 and a_2 located at coordinates C_1^i and C_2^i connecting the two sheets. Boundary conditions at these throats are derived from isometries between the two sheets. These conditions are that at the surface \mathcal{S} of each of the throats:

$$\alpha|_{\mathcal{S}} = 0 \quad (2.40)$$

$$\beta_{\parallel}|_{\mathcal{S}} = 0 \quad (2.41)$$

$$n^j \nabla_j \beta_{\perp}^i|_{\mathcal{S}} = 0 \quad (2.42)$$

$$\left(n^i \nabla_i \bar{\phi} + \frac{\bar{\phi}}{2r} \right) \Big|_{\mathcal{S}} = 0. \quad (2.43)$$

Here r denotes the radial coordinate distance from the center of the corresponding throat and n^i its unit normal. Also, $\beta_{\perp}^i = h^i_j \beta^j$ with $h_{ij} = \eta_{ij} - n_i n_j$ the induced metric in \mathcal{S} and $\beta_{\parallel} = n_i \beta^i$. Condition (2.40) on the

lapse arises from imposing anti-symmetry with respect to the isometry. Because $\bar{A}^{ij} = (\mathbb{L}\beta)^{ij}/2\alpha$, the condition $\alpha|_{\mathcal{S}} = 0$ forces one to impose $(\mathbb{L}\beta)^{ij}|_{\mathcal{S}} = 0$ in order to have regularity of the extrinsic curvature. The problem encountered by GGB was that the conditions (2.41) and (2.42) are not sufficient to guarantee that $(\mathbb{L}\beta)^{ij}|_{\mathcal{S}} = 0$. CGG designed a procedure to achieve regularity on the throats; however, Cook [24] showed that a consequence of this regularization is the introduction of constraint violations.

III. CTT-CTS MAPPING

The objective now is to find a prescription to translate between CTT and CTS data. Consider initial data $(\tilde{g}_{ij}, \tilde{K}_{ij})_{CTT}$ and $(\hat{g}_{ij}, \hat{K}_{ij})_{CTS}$ computed by the CTT and CTS methods, respectively. Without loss of generality, because of the conformal flatness and $K = 0$ assumptions, one can set:

$$\tilde{g}_{ij}|_{CTS} = \epsilon^4 \tilde{g}_{ij}|_{CTT} \quad (3.1)$$

$$\hat{A}_{ij}|_{CTS} = \hat{A}_{ij}|_{CTT} + \bar{\phi}^{-2} a_{ij}, \quad (3.2)$$

with a_{ij} a traceless tensor and ϵ a function. When rewritten in terms of CTT and CTS quantities, these relations take the following form:

$$\epsilon = \frac{\bar{\phi}}{\hat{\phi}} \quad (3.3)$$

$$\frac{(\mathbb{L}\bar{\beta})_{ij}}{2\bar{\alpha}\bar{\phi}^{-6}} = \epsilon^2 (\mathbb{L}W)_{ij} + a_{ij}. \quad (3.4)$$

with bars and hats denoting CTS and CTT quantities, respectively.

Since by construction,

$$\nabla_j (\mathbb{L}W)^{ij} = 0 \quad \text{and} \quad \nabla_j \left[\frac{(\mathbb{L}\bar{\beta})^{ij}}{2\bar{\alpha}\bar{\phi}^{-6}} \right] = 0,$$

ϵ and a_{ij} must satisfy the following condition:

$$\nabla_j a^{ij} + (\mathbb{L}W)^{ij} \nabla_j \epsilon^2 = 0. \quad (3.5)$$

Clearly, if identical data are to be produced by CTT and CTS methods, one would need to show that $\epsilon = 1$ and that the only solution to (3.5) is $a_{ij} = 0$.

The main difficulty in relating CTT and CTS data is that one not only has to establish a connection between their corresponding equations but also their asymptotic conditions as well as how the singularities are handled. Since CTT binary black hole initial data are computationally less demanding to obtain (they only require solving Eq. (2.21)), a starting point in checking whether CTT and CTS data are the same is to verify whether the CTT data satisfy the CTS conditions $\partial_t \hat{g}_{ij} = 0$ and $\partial_t K = 0$.

A. From CTT to CTS

We will concentrate attention on the steps to bring CTT data into a CTS form. That is, the initial data $(\tilde{g}_{ij}, \tilde{K}_{ij})$ are given by the CTT method, namely $\tilde{g}_{ij} = \phi^4 \eta_{ij}$ and $\tilde{K}_{ij} = \phi^{-2} (\mathbb{L}W)_{ij}$, with $(\mathbb{L}W)_{ij}$ given by (2.25) or (2.26) and ϕ computed from

$$\nabla^2 \phi = -\frac{1}{8} \phi^{-7} (\mathbb{L}W)^2. \quad (3.6)$$

To simplify notation, we have dropped the hats used to denote CTT quantities.

Satisfying the CTS condition $\partial_t K = 0$ is trivial since this condition is essentially an equation for the lapse function. Following a procedure similar to that used in deriving (2.36), with $\tilde{A}_{ij} = \phi^{-2} (\mathbb{L}W)_{ij}$ instead of $\tilde{A}_{ij} = \phi^4 (\mathbb{L}\beta)_{ij} / 2\alpha$, one obtains

$$\nabla^2(\alpha\phi) = \frac{7}{8} (\alpha\phi) \phi^{-8} (\mathbb{L}W)^2. \quad (3.7)$$

Asymptotic flatness imposes on Eqs. (3.6) and (3.7) the following conditions as $r \rightarrow \infty$:

$$n^i \nabla_i \phi = \frac{(1-\phi)}{r} \quad (3.8)$$

$$n^i \nabla_i (\alpha\phi) = \frac{[1 - (\alpha\phi)]}{r}, \quad (3.9)$$

respectively. These conditions imply that

$$\phi = 1 + \frac{a}{r} + O(r^{-2}) \quad (3.10)$$

$$\alpha\phi = 1 - \frac{b}{r} + O(r^{-2}), \quad (3.11)$$

which in turn yield

$$\begin{aligned} \alpha &= \frac{1 - a/r}{1 + b/r} + O(r^{-2}) \\ &= 1 - \frac{a+b}{2r} + O(r^{-2}). \end{aligned} \quad (3.12)$$

Above, a and b are parameters related to the ADM [5] and Komar [17] masses, respectively. In GGB, the condition for quasi-circular orbits is found by equating these two masses.

Next is the condition $\partial_t g_{ij} = 0$. Once again, a derivation similar to what was used in obtaining (2.32) yields

$$(\mathbb{L}\beta)^{ij} = 2\alpha\phi^{-6} (\mathbb{L}W)^{ij}. \quad (3.13)$$

Solving (3.13) as it stands is conceptually difficult. There are five equations for the three components of the shift vector. Thus, solutions are only possible in the particular case when the tensor $\alpha\phi^{-6} (\mathbb{L}W)^{ij}$ is purely longitudinal. A system of equations for β^i that is not over-determined is obtained by taking the divergence of (3.13):

$$\nabla_j (\mathbb{L}\beta)^{ij} = 2 (\mathbb{L}W)^{ij} \nabla_j (\alpha\phi^{-6}). \quad (3.14)$$

The potential problem of computing β^i from Eq. (3.14) is that, in general, yields

$$(\mathbb{L}\beta)^{ij} = 2\alpha\phi^{-6} (\mathbb{L}W)^{ij} + u^{ij}, \quad (3.15)$$

with $\nabla_j u^{ij} = 0$. A non-vanishing u_{ij} would imply $\partial_t g_{ij} \neq 0$. Therefore, the only possible way of reconciling CTT and CTS data is if the solution to Eq. (3.14) yields $u^{ij} = 0$. In Ref. [20], we showed that $u^{ij} \approx 0$ for binary black hole data with punctures at separations close to ISCO.

Given the asymptotic behavior of ϕ and α , as $r \rightarrow \infty$, Eq. (3.13) becomes

$$(\mathbb{L}\beta)^{ij} = 2 (\mathbb{L}W)^{ij}. \quad (3.16)$$

Therefore, $\beta^i \rightarrow 2W^i + B^i$, such that B^i is a conformal Killing vector, i.e. $(\mathbb{L}B)^{ij} = 0$. For example, in the case of binary data in a co-rotating frame,

$$\beta^i \rightarrow 2W^i + \Omega \left(\frac{\partial}{\partial \varphi_o} \right)^i. \quad (3.17)$$

In summary, given the vector W^i , the initial data is completely determined once (3.6) is solved. The solution to this equation does not require knowledge of α and β^i . The role played by Eqs. (3.7) and (3.13) is to provide coordinate conditions that recast the data into a CTS form. The lapse function is fixed by Eq. (3.7), which is derived from the condition for Σ_t to be a maximal slice. The shift vector is fixed, on the other hand, by Eq. (3.13), which is needed to impose the quasi-equilibrium condition $\partial_t g_{ij} = 0$.

B. Komar Mass and Generalized Smarr Formula

We need now to address how to fix the orbital angular velocity Ω in (3.17). In GGB, Ω fixes the boundary condition that determines the initial data. Our case is different; the initial data (ϕ, W^i) are obtained following the CTT method, so it is not until one solves for the shift vector that the issue of specifying a frame of reference emerges. If one chooses to solve for the shift with the asymptotic condition $\beta^i = 2W^i$, the data $(\phi, W^i, \alpha, \beta^i)$ should be viewed as computed in an inertial frame of reference.

One can transform these data to a rotating frame [3] by simply changing the shift vector to

$$\beta^i \rightarrow \beta^i + \Omega \left(\frac{\partial}{\partial \varphi_o} \right)^i. \quad (3.18)$$

This transformation assumes that the inertial and rotating frame are instantaneously aligned. It also implies that the lapse function, spatial metric and extrinsic curvature are unchanged.

But the question still remains about how to fix Ω . One would like in principle that

$$l^\mu = \left(\frac{\partial}{\partial t} \right)^\mu = \alpha N^\mu + \beta^\mu \quad (3.19)$$

is a Killing vector, with t the time coordinate associated with the rotating frame. If such a Killing vector exists, it implies that the physical metric and extrinsic curvature satisfy

$$\partial_t \tilde{g}_{ij} = 0 \quad (3.20)$$

$$\partial_t \tilde{K}_{ij} = 0. \quad (3.21)$$

As pointed out by GGB [7], this requirement is too strong since energy would have to be pumped continuously into the system to keep the binary at a fixed orbit, thus violating asymptotic flatness.

Instead, one can require that in the rotating frame the conformal metric and trace of the extrinsic curvature satisfy

$$\partial_t g_{ij} = 0 \quad (3.22)$$

$$\partial_t K = 0. \quad (3.23)$$

Eq. (3.22) is equivalent to the thin-sandwich condition $u_{ij} = 0$. Similarly, Eq. (3.23) is nothing other than the condition for Σ_t to be a maximal slice.

Given (3.22) and (3.23), as well as $K = 0$, the evolution equations (2.13) and (2.14) yield

$$(\tilde{\mathbb{L}}\beta)_{ij} - 2\alpha \tilde{A}_{ij} = 0 \quad (3.24)$$

$$\tilde{\nabla}^i \tilde{\nabla}_i \alpha - \alpha \tilde{A}^{ij} \tilde{A}_{ij} = 0, \quad (3.25)$$

respectively. Substitution of (3.24) into (3.25), together with the momentum constraint $\tilde{\nabla}_j \tilde{A}^{ij} = 0$, yields

$$\tilde{\nabla}^i (\tilde{\nabla}_i \alpha - \tilde{A}_{ij} \beta^j) = 0. \quad (3.26)$$

It is important to emphasize that this equation does not require conformal flatness to hold.

Integration of (3.26) over Σ_t excluding the black hole singularities (sources) yields [7]

$$\frac{1}{4\pi} \oint_{\infty} (\tilde{\nabla}_i \alpha - \tilde{A}_{ij} \beta^j) dS^i + I = 0 \quad (3.27)$$

where

$$I \equiv \frac{1}{4\pi} \sum_{A=1,2} \oint_{\mathcal{S}_A} (\tilde{\nabla}_i \alpha - \tilde{A}_{ij} \beta^j) dS^i. \quad (3.28)$$

Here \mathcal{S}_A are 2-spheres surrounding the black holes with dS^i oriented toward the interior of the black hole.

The integral in (3.27) involving the gradient of the lapse has a physical interpretation. Given a time-like Killing vector ξ^μ , the total mass (Komar mass) in a space-like hypersurface is given by [17]

$$M_{KMR} = \frac{1}{4\pi} \oint_{\mathcal{S}} \tilde{\nabla}^\mu \xi^\nu n_\mu N_\nu dS, \quad (3.29)$$

with n^μ a unit vector in Σ_t normal to a 2-surface \mathcal{S} enclosing the sources. N^μ is the time-like unit normal to Σ_t . In particular, one could take \mathcal{S} to be at spatial infinity

and $\xi^\mu \rightarrow \alpha (\partial/\partial t_o)^\mu$, with $(\partial/\partial t_o)^\mu$ the time-translation Killing vector of the flat metric. One can then show [25] that

$$M_{KMR} = \frac{1}{4\pi} \oint_{\infty} \tilde{\nabla}_i \alpha dS^i. \quad (3.30)$$

Thus, Eq. (3.27) becomes

$$M_{KMR} - \frac{1}{4\pi} \oint_{\infty} \tilde{A}_{ij} \beta^j dS^i + I = 0. \quad (3.31)$$

One must emphasize that here M_{KMR} is meant to represent the result of the integral (3.30). It does not imply the existence of a global time-like Killing vector in Σ_t . That is, in general $\partial_t \phi \neq 0$ and $\partial_t \tilde{A}_{ij} \neq 0$.

The second term in (3.31) has also a physical interpretation. If $\beta^i \rightarrow \Omega (\partial/\partial \varphi_o)^i$,

$$2\Omega J_{ADM} = \frac{1}{4\pi} \oint_{\infty} \tilde{A}_{ij} \beta^j dS^i, \quad (3.32)$$

with J_{ADM} the total angular momentum in Σ_t [5]. Therefore,

$$M_{KMR} - 2\Omega J_{ADM} + I = 0. \quad (3.33)$$

One can then use this equation to solve for Ω . However, Eq. (3.33) does not fix Ω in the sense of providing a quasi-stationary situation. Given any solution (ϕ, α, β^i) to the system of equations (3.6–3.14), one can always solve for Ω from (3.33). The value of Ω obtained in this fashion yields coordinate conditions (α, β^i) such that Eqs. (3.22) and (3.23) are satisfied. It does not, however, necessarily imply that the vector l^μ in (3.19) is an approximate helical Killing vector.

As pointed out by Cook [24], perhaps the most valuable aspect of the work by GGB is to fix Ω by requiring that the ADM and Komar masses are equal. With this condition, Eq. (3.33) becomes

$$M_{ADM} - 2\Omega J_{ADM} + I = 0, \quad (3.34)$$

with

$$M_{ADM} = -\frac{1}{2\pi} \oint_{\infty} \tilde{\nabla}_i \phi dS^i. \quad (3.35)$$

Eq. (3.34) is also known as the generalized Smarr formula [7].

The idea behind constructing data with $M_{ADM} = M_{KMR}$ is motivated by Beig's observation [26] that for stationary space-times these masses are indeed equal. Therefore, specifying Ω to fulfill $M_{ADM} = M_{KMR}$ would hopefully yield a co-rotating frame for quasi-circular orbits that minimizes a suitable norm of $\partial_t \phi$ and $\partial_t \tilde{A}_{ij}$ [20].

If the shift vector solution to Eq. (3.14) is such that a residual transverse-traceless part $u_{ij} = \partial_t g_{ij}$ is present, it is still possible to derive an expression similar to (3.34). In this case, one needs to modify I to be [20]

$$I \equiv \frac{1}{4\pi} \sum_{A=1,2} \oint_{\mathcal{S}_A} (\tilde{\nabla}_i \alpha - \tilde{A}_{ij} \beta^j) dS^i \quad (3.36)$$

$$+ \frac{1}{8\pi} \int \tilde{A}^{ij} \tilde{g}^{1/3} u_{ij} \sqrt{\tilde{g}} d^3x. \quad (3.37)$$

Even for non-vanishing u_{ij} , the condition $M_{ADM} = M_{KMR}$ can be applied. It will minimize the norm of $\partial_t g_{ij}$, in addition to those of $\partial_t \phi$ and $\partial_t \tilde{A}_{ij}$ [20]. In Ref. [19], this methodology was used to construct binary black hole sequences with punctures. The results are in close agreement with those by Baumgarte [12].

It is important to mention that in the CTS initial data construction by GGB, Eq. (3.34) is only used as a consistency check. The GGB methodology is such that part of the outcome is the rotating frame itself. As discussed before, the angular velocity Ω of the co-rotating frame enters in the boundary conditions needed to solve for the shift vector. That is, Ω is adjusted to yield $M_{ADM} = M_{KMR}$. In our approach, on the other hand, the initial data is given by the CTT method, with Ω a derived quantity. To fix $M_{ADM} = M_{KMR}$, one adjusts instead [20] the parameters a and b in (3.10) and (3.11).

Finally, if instead of $\beta^i \rightarrow \Omega (\partial/\partial\varphi_o)^i$, one has that $\beta^i \rightarrow V (\partial/\partial x_o)^i$, with $(\partial/\partial x_o)^i$ the Killing vector of the flat metric along the direction x_o^i , the integral in the second term in (3.31) has a different physical interpretation. In this case,

$$\frac{1}{4\pi} \oint_{\infty} \tilde{A}_{ij} \beta^j dS^i = 2V P_{ADM}, \quad (3.38)$$

with P_{ADM} the total linear momentum in Σ_t [5]. The Smarr formula reads in this situation

$$M_{KMR} - 2V P_{ADM} + I = 0. \quad (3.39)$$

IV. CTS PUNCTURES

We will now explicitly consider CTS data involving punctures [14]. One decomposes ϕ and $\alpha\phi$ as

$$\phi = u + \frac{1}{p} \quad (4.1)$$

$$\alpha\phi = v + \frac{1}{q}, \quad (4.2)$$

such that

$$\frac{1}{p} = \frac{a_1}{r_1} + \frac{a_2}{r_2} \quad (4.3)$$

$$\frac{1}{q} = -\frac{b_1}{r_1} - \frac{b_2}{r_2}, \quad (4.4)$$

respectively. Above, a and b are parameters and u and v regular functions. The parameter a and b can be related to the ‘‘bare’’ masses of the punctures [20].

Substitution of (4.1) and (4.2) into Eqs. (2.33) and (2.36) yields

$$\nabla^2 u = -\frac{\phi^5}{32\alpha^2} (\mathbb{L}\beta)^2 \quad (4.5)$$

$$\nabla^2 v = \frac{7}{32} \frac{\phi^6}{(\alpha\phi)} (\mathbb{L}\beta)^2. \quad (4.6)$$

For asymptotic flatness, the following Robin boundary conditions are imposed far from the holes:

$$n^i \nabla_i u = \frac{(1-u)}{r} \quad (4.7)$$

$$n^i \nabla_i v = \frac{(1-v)}{r}. \quad (4.8)$$

As pointed out in Ref. [21], the problem with punctures in the CTS method is that a natural choice is

$$\lim_{r \rightarrow \infty} \alpha = 1 \quad (4.9)$$

$$\lim_{r \rightarrow r_A} \alpha = -c_A < 0. \quad (4.10)$$

Therefore, the lapse function would necessarily have to vanish at some internal boundary. In order to have regularity of u and v , one would have to have that $(\mathbb{L}\beta)^{ij}$ vanishes at least as fast as α at that internal boundary. Imposing the vanishing of $(\mathbb{L}\beta)^{ij}$ in general requires more freedom than is available. One could in principle set $c_A < 0$. This choice, however, yields solutions far from being quasi-stationary.

If the combination of punctures and CTS seems to be intrinsically troublesome, it seems then puzzling that CTS conformal-imaging and CTT puncture binary black hole initial data sets exhibit good agreement as the separation of the binary increases. It should then be possible to translate, using the procedure described in the previous section, the CTT-puncture data into a CTS form in spite of the presence of an internal boundary where $\alpha = 0$. To demonstrate that this is the case, we consider single black hole solutions. For large separations, not only does the solution approximate that of a single, spinning black hole far away from the binary system, but it also approaches the solution of a single black hole with linear momentum near each of the black holes. Specifically, we will consider Bowen and York [22] single black hole solutions using punctures and show that it is possible to bring those solutions into a CTS form.

From (4.5), (4.6) and (3.13), the equations to be solved are:

$$\nabla^2 u = -\frac{1}{8} \frac{1}{(pu+1)^7} p^7 (\mathbb{L}W)^2 \quad (4.11)$$

$$\nabla^2 v = \frac{7}{8} \frac{(qv+1)}{(pu+1)^8} \frac{p^8}{q} (\mathbb{L}W)^2 \quad (4.12)$$

$$(\mathbb{L}\beta)^{ij} = 2 \frac{(qv+1)}{(pu+1)^7} \frac{p^7}{q} (\mathbb{L}W)^{ij}. \quad (4.13)$$

with $(\mathbb{L}W)^{ij}$ given by (2.25) or (2.26). Notice that because $(\mathbb{L}W)^{ij}$ is linear in the momentum, we will only consider perturbative solutions [27, 28] to second order in the momentum for u and v and linear order for β^i .

Therefore,

$$\nabla^2 u = -\frac{1}{8} \frac{\bar{r}^7}{(\bar{r}+1)^7} (\mathbb{L}W)^2 \quad (4.14)$$

$$\nabla^2 v = \frac{7}{8} \frac{(\bar{r}-\bar{b})\bar{r}^7}{(\bar{r}+1)^8} (\mathbb{L}W)^2 \quad (4.15)$$

$$(\mathbb{L}\beta)^{ij} = 2 \frac{(\bar{r}-\bar{b})\bar{r}^6}{(\bar{r}+1)^7} (\mathbb{L}W)^{ij}, \quad (4.16)$$

where over-bars here denote scaling with respect to the parameter a (i.e. $\bar{r} \equiv r/a$, $\bar{b} = b/a$, $\bar{P} = P/a$ and $\bar{J} = J/a^2$).

A. Spinning Bowen-York Black Hole

For a spinning Bowen-York black hole [22], the only non-vanishing component of W^i and $(\mathbb{L}W)_{ij}$ are

$$W^\varphi = -\frac{J}{r^3} \quad (4.17)$$

$$(\mathbb{L}W)_{r\varphi} = \frac{3J}{r^2} \sin^2 \theta, \quad (4.18)$$

where J is the total angular momentum. Therefore,

$$(\mathbb{L}W)^2 = \frac{18J^2}{r^6} \sin^2 \theta = \frac{12J^2}{r^6} [P_0(\mu) - P_2(\mu)], \quad (4.19)$$

where $\mu \equiv \cos \theta$ and P_l are Legendre polynomials. Substitution of (4.19) into Eqs. (4.14–4.16) yields

$$\nabla^2 u = -\frac{3}{2} \frac{J^2 r}{(r+1)^7} [P_0(\mu) - P_2(\mu)] \quad (4.20)$$

$$\nabla^2 v = \frac{21}{2} \frac{J^2 r (r-b)}{(r+1)^8} [P_0(\mu) - P_2(\mu)] \quad (4.21)$$

$$\partial_r \beta^\varphi = 6J r^2 \frac{(r-b)}{(r+1)^7}. \quad (4.22)$$

To simplify notation, we have dropped the over-bars, and rescaled β^φ as $\beta^\varphi a$.

Regular solutions to (4.20)-(4.22) are

$$u(r, \mu) = J^2 [u_0(r) P_0(\mu) + u_2(r) r^2 P_2(\mu)] \quad (4.23)$$

$$v(r, \mu) = J^2 [v_0(r) P_0(\mu) + v_2(r) r^2 P_2(\mu)] \quad (4.24)$$

$$\beta^\varphi(r) = J \left[\frac{-2}{(r+1)^3} + \frac{3(b+3)}{2(r+1)^4} - \frac{6(2b+3)}{5(r+1)^5} + \frac{(b+1)}{(r+1)^6} + \frac{(1-b)}{10} \right] \quad (4.25)$$

where

$$40u_0(r) = \frac{1}{(r+1)} + \frac{1}{(r+1)^2} + \frac{1}{(r+1)^3} - \frac{4}{(r+1)^4} + \frac{2}{(r+1)^5} \quad (4.26)$$

$$20u_2(r) = \frac{-1}{(r+1)^5} \quad (4.27)$$

$$40v_0(r) = \frac{(3b-4)}{(r+1)} + \frac{(3b-4)}{(r+1)^2} + \frac{(3b-4)}{(r+1)^3} + \frac{(3b+31)}{(r+1)^4} - \frac{(18b+32)}{(r+1)^5} + \frac{10(b+1)}{(r+1)^6} \quad (4.28)$$

$$20v_2(r) = \frac{r(6-b) - 6b + 1}{(r+1)^6}. \quad (4.29)$$

These solutions have the following asymptotic form when $r \rightarrow \infty$:

$$\phi = 1 + \frac{1}{r} \left(1 + \frac{J^2}{40} \right) \quad (4.30)$$

$$\alpha = 1 - \frac{1}{r} \left[b + 1 + \frac{J^2(5-3b)}{40} \right] \quad (4.31)$$

$$\beta^\varphi = J \left[\frac{(1-b)}{10} - \frac{2}{r^3} \right] = \frac{J(1-b)}{10} + 2W^\varphi. \quad (4.32)$$

Furthermore, integration constants for β^φ have been chosen such that $\beta^\varphi(0) = 0$. From Eqs. (3.35) and (3.30), the ADM and Komar masses are respectively

$$M_{ADM} = 2 + \frac{J^2}{20} \quad (4.33)$$

$$M_{KMR} = b + 1 + \frac{J^2(5-3b)}{40} \quad (4.34)$$

On the other hand, it is not difficult to show that near the puncture the integral I , defined by (3.28), yields

$$I = -[1 + b + J^2(bu_0(0) + v_0(0))] = -\left[1 + b + \frac{J^2(5b-3)}{40} \right]. \quad (4.35)$$

Similarly from (3.32),

$$\Omega = \frac{J(1-b)}{10}, \quad (4.36)$$

which is consistent with our requirement that asymptotically $\beta^\varphi \rightarrow \Omega$. Clearly, the computed values for M_{KMR} , I and Ω satisfy the Smarr formula $M_{KMR} - 2\Omega J + I = 0$. In addition, to satisfy the condition $M_{ADM} = M_{KMR}$, one needs to set $b = 1$, which in turn implies that $\Omega = 0$.

B. Boosted Bowen-York Black Hole

The only non-vanishing components of W^i and $(\mathbb{L}W)_{ij}$ for a boosted Bowen-York black hole [22] are:

$$\begin{aligned} W^r &= -2 \frac{P}{r} \cos \theta \\ W^\theta &= \frac{7}{4} \frac{P}{r^2} \sin \theta \\ (\mathbb{L}W)_{rr} &= 3 \frac{P}{r^2} \cos \theta \\ (\mathbb{L}W)_{r\theta} &= -\frac{3}{2} \frac{P}{r} \cos \theta \\ (\mathbb{L}W)_{\theta\theta} &= -\frac{3}{2} P \cos \theta \\ (\mathbb{L}W)_{\varphi\varphi} &= -\frac{3}{2} P \cos \theta \sin^2 \theta, \end{aligned} \quad (4.37)$$

where the linear momentum is assumed to point along the positive z axis and have magnitude P .

With the above expression, the term $(\mathbb{L}W)^2$ takes the form

$$(\mathbb{L}W)^2 = \frac{3}{2} \frac{P}{r^4} [5 P_0(\mu) + 4 P_2(\mu)]. \quad (4.39)$$

The equations to be solved for u and v in this case are:

$$\nabla^2 u = -\frac{3}{16} \frac{P^2 r^3}{(r+1)^7} [5 P_0(\mu) + 4 P_2(\mu)] \quad (4.40)$$

$$\nabla^2 v = \frac{21}{16} \frac{P^2 r^3 (r-b)}{(r+1)^8} [5 P_0(\mu) + 4 P_2(\mu)], \quad (4.41)$$

and for the shift vector

$$r \partial_r \left(\frac{\beta^r}{r} \right) - \partial_\theta \beta^\theta = 9 \frac{P r^4 (r-b)}{(r+1)^7} \cos \theta \quad (4.42)$$

$$r^2 \partial_r \beta^\theta + \partial_\theta \beta^r = -3 \frac{P r^5 (r-b)}{(r+1)^7} \sin \theta. \quad (4.43)$$

In the equations above, we have introduced the same scaling with respect to the parameter a as in the previous section.

Regular solutions to (4.40)–(4.43) are:

$$u(r, \mu) = P^2 [u_0(r) P_0(\mu) + u_2(r) P_2(\mu)] \quad (4.44)$$

$$v(r, \mu) = P^2 [v_0(r) P_0(\mu) + v_2(r) P_2(\mu)] \quad (4.45)$$

$$\beta^r(r, \theta) = P R(r) \cos \theta \quad (4.46)$$

$$\beta^\theta(r, \theta) = P S(r) \frac{1}{r} \sin \theta, \quad (4.47)$$

where

$$\begin{aligned} \frac{32}{5} u_0(r) &= \frac{1}{(r+1)} - \frac{2}{(r+1)^2} + \frac{2}{(r+1)^3} \\ &\quad - \frac{1}{(r+1)^4} + \frac{1}{5(r+1)^5} \end{aligned} \quad (4.48)$$

$$\begin{aligned} 80 r u_2(r) &= \frac{15}{(r+1)} + \frac{132}{(r+1)^2} \\ &\quad + \frac{53}{(r+1)^3} + \frac{96}{(r+1)^4} \\ &\quad + \frac{82}{(r+1)^5} + \frac{84}{r(r+1)^5} \\ &\quad - \frac{84}{r^2} \ln(r+1) \end{aligned} \quad (4.49)$$

$$\begin{aligned} \frac{32}{5} v_0(r) &= \frac{(b-6)}{(r+1)} + \frac{(b+15)}{(r+1)^2} \\ &\quad - \frac{(6b+20)}{(r+1)^3} + \frac{(8b+15)}{(r+1)^4} \\ &\quad - \frac{(23b+30)}{5(r+1)^5} + \frac{(b+1)}{(r+1)^6} \end{aligned} \quad (4.50)$$

$$\begin{aligned} 80 r^2 v_2(r) &= -\frac{(201b+1020)}{(r+1)} + \frac{(275b+825)}{(r+1)^2} \\ &\quad - \frac{(287b+588)}{(r+1)^3} + \frac{(185b+283)}{(r+1)^4} \\ &\quad - \frac{(66b+80)}{(r+1)^5} + \frac{10(b+1)}{(r+1)^6} \\ &\quad + \frac{84}{r} (b+8) \ln(r+1) - 105 \end{aligned} \quad (4.51)$$

$$\begin{aligned} R(r) &= \frac{1}{(r+1)^6} \left[\frac{1}{8}(b-5) + \frac{3}{4}(b-5)r \right. \\ &\quad + \frac{1}{80}(151b-751)r^2 \\ &\quad + \frac{1}{40}(103b-503)r^3 \\ &\quad + \frac{3}{16}(11b-51)r^4 - 4r^5 \left. \right] \\ &\quad - \frac{1}{8}(b-5) \end{aligned} \quad (4.52)$$

$$\begin{aligned} S(r) &= \frac{1}{(r+1)^6} \left[-\frac{1}{8}(b-5) - \frac{3}{4}(b-5)r \right. \\ &\quad - \frac{1}{80}(149b-749)r^2 \\ &\quad - \frac{1}{40}(97b-497)r^3 \\ &\quad - \frac{3}{16}(9b-49)r^4 + \frac{7}{2}r^5 \left. \right] \\ &\quad + \frac{1}{8}(b-5). \end{aligned} \quad (4.53)$$

As $r \rightarrow \infty$, these solutions have the following form:

$$\phi = 1 + \frac{1}{r} \left(1 + \frac{5P^2}{32} \right) \quad (4.54)$$

$$\alpha = 1 - \frac{1}{r} \left[b + 1 + \frac{5P^2(7-b)}{32} \right] \quad (4.55)$$

$$\begin{aligned} \beta^r &= -P \left[\frac{(b-5)}{8} + \frac{4}{r} \right] \cos \theta \\ &= -P \frac{(b-5)}{8} \cos \theta + 2W^r \end{aligned} \quad (4.56)$$

$$\begin{aligned} \beta^\theta &= P \left[\frac{(b-5)}{8} + \frac{7}{2r} \right] \frac{\sin \theta}{r} \\ &= P \frac{(b-5)}{8} \frac{\sin \theta}{r} + 2W^\theta. \end{aligned} \quad (4.57)$$

From (4.56) and (4.57), one has that asymptotically

$$\beta^i = \frac{(5-b)}{8} P^i + 2W^i, \quad (4.58)$$

where W^i is given by (2.23).

From Eqs. (3.35) and (3.30), the ADM and Komar masses are respectively

$$M_{ADM} = 2 + \frac{5P^2}{16} \quad (4.59)$$

$$M_{KMR} = b + 1 + \frac{5P^2(7-b)}{32}, \quad (4.60)$$

and from (3.32),

$$V = \frac{(5-b)}{8} P. \quad (4.61)$$

At the puncture, it is not difficult to show that

$$\begin{aligned} I &= - \left[1 + b + P^2 (b u_0(0) + v_0(0)) \right] \\ &= - \left[1 + b + \frac{P^2(3b-5)}{32} \right]. \end{aligned} \quad (4.62)$$

It follows then that M_{KMR} , I and V above satisfy, as in the case of a spinning puncture, the Smarr relationship $M_{KMR} - 2VP + I = 0$. If in addition one imposes the condition $M_{ADM} = M_{KMR}$, then $b = 1 - 20P^2/32 + O(P^4)$ and $V = P/2 + O(P^3)$.

C. Approximate Killing Vectors

In the previous two sections, we showed that it is possible, at least at the perturbative level, to bring single, spinning or boosted CTT-punctures into a CTS form. By construction, the data satisfy the conditions $\partial_t g_{ij} = 0$ and $\partial_t K = 0$. Furthermore, in these cases the problems associated with the vanishing of the lapse are avoided. What remains is to investigate how close the data come to satisfying the conditions $\partial_t \phi = 0$ and $\partial_t \tilde{A}_{ij} = 0$, conditions necessary for the existence of an exact Killing vector.

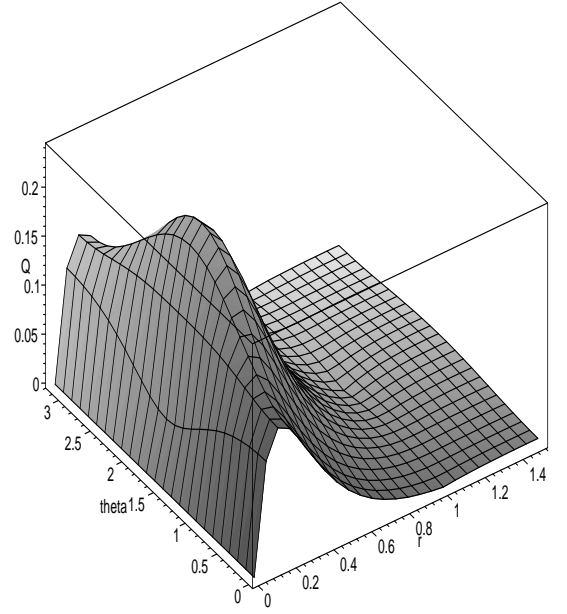


FIG. 1: Surface plot of $Q \equiv (\partial_t \tilde{A}_{ij} \partial_t \tilde{A}_{kl} g^{ik} g^{jl})^{1/2}$ for a spinning puncture in units of J^2 .

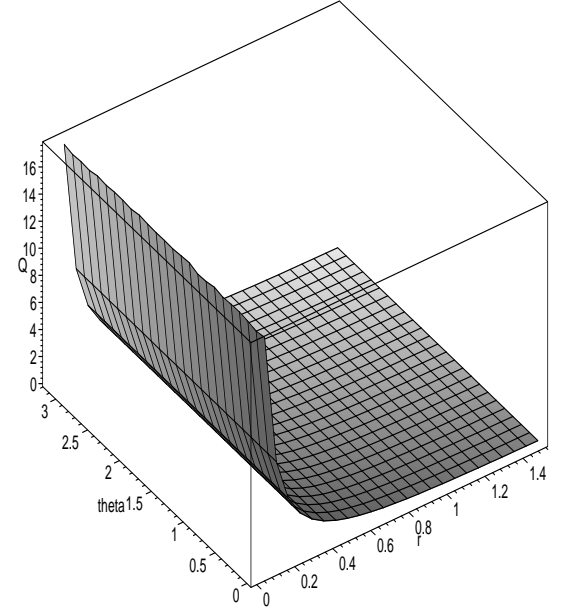


FIG. 2: Surface plot of $Q \equiv (\partial_t \tilde{A}_{ij} \partial_t \tilde{A}_{kl} g^{ik} g^{jl})^{1/2}$ for a boosted puncture in units of P^2 .

From Eqs. (2.12) and (2.15), we have that

$$\partial_t \phi = \beta^i \nabla_i \phi + \frac{1}{6} \phi \nabla_i \beta^i \quad (4.63)$$

$$\begin{aligned} \partial_t \tilde{A}_{ij} &= \mathcal{L}_\beta \tilde{A}_{ij} - 2\alpha \tilde{A}_{ik} \tilde{A}^k{}_j \\ &\quad + [\alpha \tilde{R}_{ij} - \tilde{\nabla}_i \tilde{\nabla}_j \alpha]^{TF}, \end{aligned} \quad (4.64)$$

where the condition $K = 0$ has been used. Because the solutions in Secs. IV A and IV B are up to second order in the momentum (linear or angular) for ϕ and α and first

order for β^i , one only needs to focus attention to $\partial_t\phi$ and $\partial_t\tilde{A}_{ij}$ up to second order in the momentum.

From Sec. IV A, we have that for a spinning puncture the solutions are independent of the coordinate φ and the only non-vanishing component of the shift vector is β^φ . It is then clear from (4.63) that $\partial_t\phi = 0$. For the case of a boosted puncture, on the other hand, one has that

$$\partial_t\phi = \frac{P}{80} \frac{r \cos\theta}{(r+1)^5} (b-1)(10r^2 + 5r + 1) + O(P^3). \quad (4.65)$$

At the end of Sec. IV B, we saw that in order to have $M_{ADM} = M_{KMR}$, one needs $b = 1 + O(P^2)$; therefore, $\partial_t\phi = O(P^3) \approx 0$. To second order in the momentum, $\partial_t\phi$ vanishes identically.

To zero order in P or J , Eq. (4.64) equation reads

$$\partial_t\tilde{A}_{ij} = \frac{(b-1)}{r(r+1)^2} \text{diag}[-2, r^2, r^2 \sin^2\theta], \quad (4.66)$$

Therefore, $\partial_t\tilde{A}_{ij} = 0$ since to this order $M_{ADM} = M_{KMR}$ yields $b = 1$. To first order in P and J , Eq. (4.64) vanishes identically.

On the other hand, to second order in J , we have that for a spinning puncture, even for $b = 1$, the only vanishing components are $\partial_t\tilde{A}_{r\varphi}$ and $\partial_t\tilde{A}_{\theta\varphi}$. Similarly, to second order in P , these same components of $\partial_t\tilde{A}_{ij}$ are the only ones vanishing, even if $b = 1 - 20P^2/32$ as required by $M_{KMR} = M_{ADM}$. The non-vanishing of $\partial_t\tilde{A}_{ij}$ is more apparent from Fig. 1 and 2 where we plot the quantity $Q \equiv (\partial_t\tilde{A}_{ij}\partial_t\tilde{A}_{kl}g^{ik}g^{jl})^{1/2}$ as a function of the coordinates r and θ for both cases.

Having $\partial_t\tilde{A}_{ij} \neq 0$ to second order on P and J implies that the Bowen-York puncture solutions do not have an

exact Killing vector to this order. This is consistent with the results in Refs. [27, 28] showing that Bowen-York initial data for a spinning or boosted black hole do not represent a constant-time slice of a Kerr or a boosted Schwarzschild black hole, respectively.

V. CONCLUSIONS

We have considered single boosted or spinning black hole punctures of the Bowen-York type and demonstrated that, at the perturbative level, it is possible to establish a direct connection between CTT and CTS initial data satisfying the conditions used by GGB needed for the existence of an approximate Killing vector. Since for widely separated binary systems the black holes can be viewed as nearly isolated, our results contribute to explaining the agreement between CBB and GGB binary data sets as the separation of the binary system increases.

VI. ACKNOWLEDGMENTS

This work was supported by NSF grants PHY-9800973 and PHY-0114375. Special thanks to Abhay Ashtekar, Bernd Brügmann and Wolfgang Tichy for helpful discussions. Thanks also to Bernard Kelly for carefully reviewing the manuscript. Work supported in part by the Center for Gravitational Wave Physics funded by the National Science Foundation under Cooperative Agreement PHY-0114375.

-
- [1] L.P. Grishchuk, et al., *Physics-Uspekhi* **171**, 3 (2001).
 - [2] M. Shibata and K. Uryu, *Phys. Rev. D* **61**, 064001 (2000); M. Shibata and K. Uryu, *Prog. Theor. Phys.* **107**, 265 (2002).
 - [3] M. D. Duez, P. Marronetti, S. L. Shapiro and T. W. Baumgarte, *Phys. Rev. D* **67**, 024004 (2003).
 - [4] B. Brügmann, *Int. J. Mod. Phys. D* **8**, 85 (1999); M. Alcubierre et al., *Phys. Rev. Lett.* **87**, 271103 (2001); J. Baker et al., *Phys. Rev. D* **87**, 121101 (2001); S. Brandt et al., *Phys. Rev. D* **85**, 5496 (2000).
 - [5] J. York, in *Sources of Gravitational Radiation*, edited by L. Smarr (Cambridge University Press, Cambridge, 1979), pp.83-126.
 - [6] J. Wilson and G. Mathews, *Phys. Rev. Lett.* **75**, 4161 (1995).
 - [7] E.ourgoulhon, P. Grandclement and S. Bonazzola *Phys. Rev. D* **65**, 044020 (2002).
 - [8] J.W. York, Jr., *Phys. Rev. Lett.* **82**, 1350 (1999).
 - [9] G.B. Cook, *Phys. Rev. D* **50**, 5025 (1994).
 - [10] R. Arnowitt, S. Deser and C.W. Misner, in *Gravitation: An Introduction to Current Research*, edited by L. Witten (John Wiley, New York, 1962), pp. 227-265.
 - [11] A. Ashtekar, C. Beetle, S. Fairhurst, *Class. Quantum Grav.* **16**, L1 (1999).
 - [12] T.W. Baumgarte, *Phys. Rev. D* **62**, 024018 (2000).
 - [13] B.D. Baker, gr-qc/0205082.
 - [14] S. Brandt and B. Brügmann, *Phys. Rev. Lett.* **78**, 3606 (1997).
 - [15] P. Grandclement, E.ourgoulhon and S. Bonazzola, *Phys. Rev. D* **65**, 044021 (2002).
 - [16] L.Blanchet, *Phys. Rev. D* **65**, 124009 (2002); T.Damor, E.ourgoulhon and P. Grandclement, *Phys. Rev. D* **66**, 24007 (2002).
 - [17] A. Komar, *Phys. Rev.* **113**, 934 (1959).
 - [18] M.L. Skoge and T.W. Baumgarte, *Phys. Rev. D* **66**, 107501 (2002).
 - [19] W. Tichy and B. Brügmann, gr-qc/0307027.
 - [20] B. Brügmann, W. Tichy and P. Laguna, *Phys. Rev. D* **67**, 064008 (2003).
 - [21] M.D. Hannam, C.R. Evans, G.B. Cook, T.W. Baumgarte, *Phys. Rev. D* **68**, 064003 (2003).
 - [22] J. Bowen and J.W. York, Jr., *Phys. Rev. D* **21**, 2047 (1980).
 - [23] H. P. Pfeiffer and J. W. York, Jr., *Phys. Rev. D* **67**,

- 044022 (2003).
- [24] G.B. Cook, Phys. Rev. D **65**, 084003 (2002).
- [25] E. Gourgoulhon and S. Bonazzola, Class. Quantum Grav. **11**, 443 (1994)
- [26] R. Beig, Phys. Lett. **69A**, 153 (1978)
- [27] R.J. Gleiser, C.O. Nicasio, R.H. Price and J. Pullin, Phys. Rev. D **57**, 3401 (1998).
- [28] R.J. Gleiser, G. Khanna and J. Pullin, Phys. Rev. D **66**, 024035 (2002).